CHINESE OPTICS LETTERS

Vol. 19, No. 4 | April 2021

High-power, ultra-broadband supercontinuum source based upon 1/1.5 μm dual-band pumping

Yihuai Zhu (朱逸怀)[1,†], Zhijian Zheng (郑志坚)[1,2,†], Xiaogang Ge (葛小钢)[1], Geguo Du (杜戈果)[3], Shuangchen Ruan (阮双琛)[1,2], Chunyu Guo (郭春雨)[1*], Peiguang Yan (闫培光)[1], Ping Hua (华 萍)[1], Linzhong Xia (夏林中)[4], and Qitao Lü (吕启涛)[5]

[1] Shenzhen Key Laboratory of Laser Engineering, Key Laboratory of Advanced Optical Precision Manufacturing Technology of Guangdong Higher Education Institutes, Guangdong Provincial Key Laboratory of Micro/Nano Optomechatronics Engineering, College of Physics and Optoelectronic Engineering, Shenzhen University, Shenzhen 518060, China

[2] College of New Materials and New Energies, Shenzhen Technology University, Shenzhen 518118, China

[3] College of Electronics and Information Engineering, Shenzhen University, Shenzhen 518060, China

[4] Shenzhen Institute of Information Technology, Shenzhen 518172, China

[5] Han's Laser Technology Industry Group Co., Ltd., Shenzhen 518057, China

*Corresponding author: cyguo@szu.edu.cn

Received August 7, 2020 | Accepted October 19, 2020 | Posted Online January 7, 2021

We experimentally demonstrate an all-fiber supercontinuum source that covers the spectral region ranging from visible to mid-infrared. The ultra-broadband supercontinuum is realized by pumping a cascaded photonic crystal fiber and a highly nonlinear fiber with a 1/1.5 μm dual-band pump source. A maximum output power of 9.01 W is achieved using the system, which is the highest power ever achieved from a supercontinuum source spanning from the visible to mid-infrared.

Keywords: fiber lasers; supercontinuum generation; nonlinear optics.
DOI: 10.3788/COL202119.041403

1. Introduction

Supercontinuum sources are demanded in a range of applications such as remote sensing[1], biomedical imaging[2–4], and military countermeasures[5]. Hitherto, the dominant approach for supercontinuum generation is to pump a nonlinear medium [in most cases, highly nonlinear fibers (HNLFs)] using a pulsed laser[6,7]. In order to realize a broadband supercontinuum, the pump wavelength is desired to be within the anomalous dispersion region and close to the zero dispersion wavelength (ZDW) of the HNLFs, whereby the pulses generated by the pump laser can easily extend into the long-wavelength region through soliton self-frequency shift (SSFS) and extend into the short-wavelength region through group-velocity-matched dispersive wave.

For covering different spectral regions, the supercontinuum sources can be pumped at various wavelengths: 1 μm, 1.5 μm, and 2 μm. In the 1 μm pumping scheme, ytterbium-doped fiber lasers (YDFLs) are the most popular pump sources, and silica-based photonic crystal fibers (PCFs) with ZDWs in the short-wavelength tail of the near-infrared (IR) are a common nonlinear medium. Thanks to the outstanding scalability of YDFLs, the 1 μm pumped supercontinuum sources are capable of achieving very high output powers, and their spectra usually extend into the visible or even ultra-violet (UV) region. Chen *et al.* reported a 39 W supercontinuum source with a spectrum spanning 400–2250 nm[8]. Hu *et al.* reported a 49.5 W supercontinuum source with a spectrum ranging from 500 nm to 1700 nm[9]. A UV-enhanced supercontinuum with a short-wavelength edge at 370 nm was demonstrated by Gao *et al.*[10]. The output power of UV-enhanced supercontinuum sources can be as high as 80.8 W[11–13]. The 1 μm pumped system with hundred-watt-level output was also reported previously[14]. Despite the impressive progress in power scaling, the intrinsic drawback of 1 μm pumped supercontinuum sources is that the long-wavelength coverage of their spectra is restricted in the near-IR region, owing to the limited shift range of SSFS and the strong absorption loss of silica fibers.

Regarding 1.5 μm and 2 μm pumping schemes, erbium/ytterbium-codoped fiber lasers (EYDFLs) and thulium-doped fiber lasers (TDFLs) are used as pump sources, and dispersion-matched HNLFs with ZDWs in the long-wavelength tail of the near-IR are employed as a nonlinear medium. The 1.5 μm and 2 μm pumped supercontinuum sources can provide spectral coverage spanning mid-IR, and, thus, the absorption loss of fibers in the mid-IR region has to be taken into consideration. The issue is solved by using very short silica HNLFs or

directly using soft-glass fibers, which feature low absorption in the mid-IR region. Nicholson *et al.* reported a 1.5 μm pumped supercontinuum source spanning 850–2600 nm, which uses a short piece of silica HNLF as a nonlinear medium[15]. Xia *et al.* reported a low-power (27 mW) supercontinuum source ranging from 800 nm to 3000 nm, and a high-power (5.4 W) supercontinuum source ranging from 800 nm to 2800 nm. Both systems are realized by pumping a short piece of silica HNLF with a 1.5 μm EYDFL[16]. By replacing the silica HNLF with a fluoride one, the output power of the system reported by Xia *et al.* in Ref. [16] can be further scaled to 10.5 W, and the long-wavelength coverage is extended to 4000 nm[17]. With respect to the 2 μm pumped systems, fluoride HNLF is the favorite nonlinear medium. The 2 μm pumped supercontinuum sources is capable of achieving mid-IR coverage up to 4700 nm, and their output powers can be as high as 15.2 W[18–21]. Recently, high-concentration germania-doped silica fibers and pure germania-core fibers are found to be good alternatives to the nonlinear medium for supercontinuum generation in the mid-IR region. The spectra of the supercontinuum sources using such fibers can extend to 3200 nm, and their output powers can be scaled to 10 W[22–24].

As mentioned before, a supercontinuum source pumped at the longer wavelengths (e.g., 1.5 μm and 2 μm) can produce spectra spanning the mid-IR. However, such performance is achieved at the cost of the spectral coverage in the visible region. In most reported cases, the short-wavelength boundaries of the 1.5 μm or 2 μm pumped systems are located at the wavelengths longer than 800 nm. At present, the realization of a supercontinuum spanning from the visible to mid-IR is still challenging. A potential approach to improve the spectral coverage of supercontinuum sources is to apply multi-wavelength lasers[25] as pumps. In this Letter, we demonstrate an ultra-broadband supercontinuum source that spans from 500 nm to 3000 nm. The system is based upon a particular dual-band pumping scheme, in which the nonlinear medium is pumped with a 1/1.5 μm dual-band master oscillator power amplifier (MOPA) system. The nonlinear medium is the cascade of a PCF and an HNLF. Under maximum pump power, the supercontinuum source produces an output power of 9.01 W, which is, to the best of our knowledge, the highest power realized by supercontinuum sources covering from the visible to mid-IR.

2. Experimental Setup

The schematic of the all-fiber 1/1.5 μm dual-band pumped supercontinuum source is presented in Fig. 1(a). The 1 μm seed laser is a semiconductor saturable absorber mirror (SESAM)-based passively mode-locked YDFL with a central wavelength of 1063.8 nm, of which the maximum average power is 2 mW. The repetition rate and pulse duration of the 1 μm seed laser are 50.3 MHz and 7.75 ps, respectively. The 1.5 μm band seed source is a directly electrically modulated semiconductor laser diode (LD) with a central wavelength of 1548 nm. A pulsed electrical signal is applied to modulate the LD to generate a

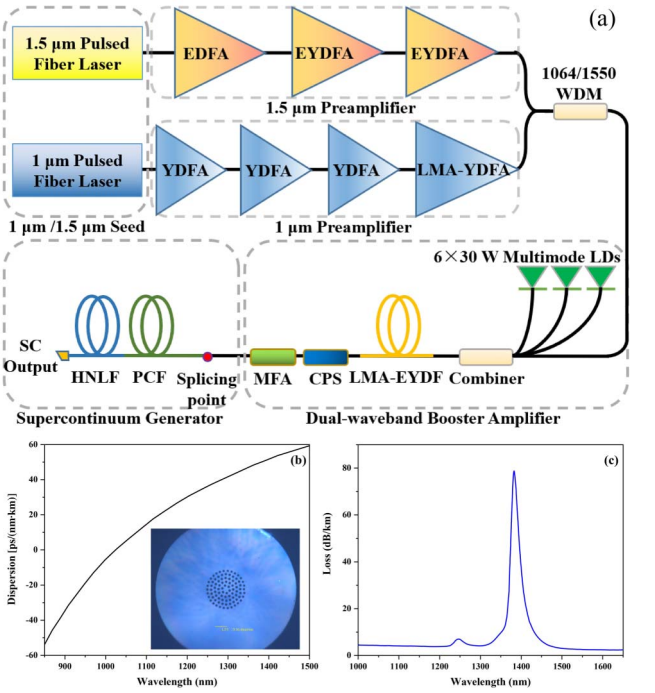

Fig. 1. (a) Experimental setup. WDM, wavelength division multiplexer; LD, laser diode pump; CPS, cladding power stripper; MFA, mode field adapter; PCF, photonic crystal fiber; HNLF, highly nonlinear fiber; SC, supercontinuum. (b) Calculated dispersion curve. The inset shows the end face of the PCF. (c) Measured transmission loss of the PCF.

1.5 μm pulse laser with 1 MHz repetition rate and 2 ns pulse duration. Since the duty cycle of the modulation signal is low, the output power is only 10 μW. Both seed lasers are amplified with multi-stage MOPAs, which employ configurations similar to the systems reported in Ref. [26]. The amplified 1/1.5 μm radiations are combined in a 1064/1550 nm wavelength division multiplexer (WDM). The mixed 1/1.5 μm radiation is subsequently injected into a booster amplifier via the signal port of a high-power $(6+1)\times 1$ combiner. The booster amplifier comprises a 1-m-long large mode area (LMA) erbium/ytterbium-codoped fiber (EYDF), which is pumped by six 976 nm LDs. The LMA EYDF is with a core/cladding diameter of 25/300 μm, a core/cladding numerical aperture (NA) of 0.09/0.46, and a cladding absorption rate of 15 dB/m at 976 nm. A high-power cladding power stripper (CPS) is used to strip the residual pump. To eliminate the high-order mode and realize mode field matching, a mode field adapter (MFA) is inserted between the booster amplifier and the supercontinuum generator. Fibers of the input/output ports of the MFA are a passive LMA fiber (core/cladding diameter: 25/300 μm, core/cladding NA: 0.09/0.46) and an HI1060 fiber (core diameter: 6 μm, core NA: 0.14), respectively. The amplified 1/1.5 μm dual-band pump is injected into the supercontinuum generator through the MFA. In the supercontinuum generator, two cascaded silica fibers are used as nonlinear medium. The first fiber (which is directly spliced to the MFA) is a PCF fabricated by Yangtze Optical Fibre and Cable Company Ltd. The PCF has a core

diameter of 4.7 μm, an air hole diameter of 1.9 μm, and a pitch of 3.3 μm. The calculated dispersion curve with an inserted cross-sectional geometry of the PCF is shown in Fig. 1(b). The nonlinear coefficient and mode field diameter (MFD) of the PCF at 1060 nm are 11 $W^{-1} \cdot km^{-1}$ and 3.9 μm, respectively[27]. Figure 1(c) shows that the transmission loss of the PCF is as low as 5 dB/km in the range of 1–1.65 μm, except for the water absorption peak at 1.36 μm (~80 dB/km). The second fiber is a silica HNLF. The HNLF has a core diameter of 3.4 μm. The nonlinear coefficient of the HNLF at 1550 nm is 10 $W^{-1} \cdot km^{-1}$. The ZDWs of the PCF and the HNLF are, respectively, 1030 nm and 1550 nm, which match well with the 1/1.5 μm dual-band pump. The splicing loss of HI1060-PCF and PCF-HNLF is 0.36 and 0.46 dB, respectively. For achieving an optimized performance of the system, the lengths of the PCF and the HNLF are adjustable. In experiments, the splicing points, fiber components (combiner, CPS, and MFA), as well as the active fiber in the booster amplifier are water-chilled using customized heat sinks to prevent thermal damage induced by the high-power operation.

The output spectra of the dual-band pumped supercontinuum source are acquired using an optical spectrum analyzer (OSA, Yokogawa AQ6373, operating range: 350–1200 nm, resolution: 0.02 nm) and a Fourier transform IR spectrometer (Bruker Tensor27, operating range: 1000–5000 nm, resolution: 1 cm^{-1}). The visible region is acquired with the OSA, whilst the mid-IR region is acquired with the spectrometer. The spectra acquired with the two devices are finally combined in a single diagram, with a joint point at the wavelength of 1100 nm.

3. Results and Discussion

In experimental works, we first investigate the characteristics of the pump laser, that is, the output from the final stage (i.e., booster amplifier) of the MOPA system. The highest power of the mixed 1/1.5 μm radiation to be sent into the supercontinuum generator is 23 W, which is achieved under the maximum available pump power (150 W) provided by the 976 nm LDs. It should be noted that the power is measured at the output port of the MFA, that is, the loss induced by mode field mismatch is already taken into account. The specific powers of the 1 μm and the 1.5 μm radiation are 10.8 W and 12.2 W, respectively. The spectral evolution of the mixed pump with the rising powers is shown in Fig. 2(a). As the output power increases, the 1 μm peak broadens slightly, whilst the 1.5 μm peak exhibits strong expansion towards the long-wavelength region. The reason for the spectral broadening of the 1.5 μm peak is modulation instability and Raman-induced frequency red-shift in the anomalous dispersion region of the output fiber of the MFA. The modulation instability leads to the splitting of the 1.5 μm pulses. The Raman-induced SSFS promotes a red-shift. The spectrum of the 1.5 μm radiation consequently extends into the long-wavelength region. As shown in Fig. 2(b), with the increase of pump power, the slope efficiency of 1 μm radiation increases from 6.8% to 9.4%, while the slope efficiency of 1.5 μm

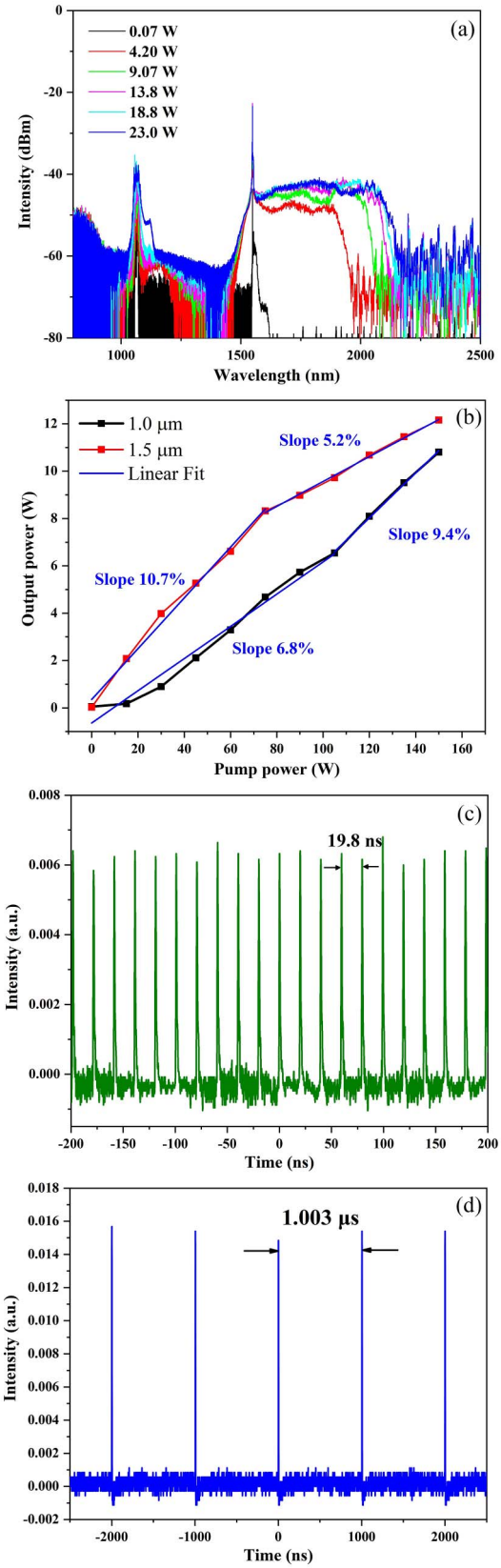

Fig. 2. (a) Spectral evolution of the 1/1.5 μm mixed pump with various output powers. (b) Output powers of the 1/1.5 μm radiations from the dual-band fiber amplifier. Output pulse trains at (c) 1 μm and (d) 1.5 μm at the maximum output power.

radiation decreases from 10.7% to 5.2%, like the trend in Ref. [26]. Output pulse trains of 1 μm and 1.5 μm radiation at the maximum output power are shown in Figs. 2(c) and 2(d), respectively.

As described above, the PCF spliced with the output port of the MFA possesses a ZDW (1030 nm) close to the central wavelength of the 1 μm pump (1063.8 nm). As a result, the PCF is pumped at the ZDW (by the 1 μm pump) and in the anomalous dispersion region (by the 1.5 μm pump) simultaneously. The output spectra measured after the PCF are presented in Fig. 3, which are measured with a variety of fiber lengths (1.4 m, 5 m, and 8 m).

The highest output power is achieved when the length of the PCF is 1.4 m. In such a case, the 10.7 W supercontinuum with a spectrum ranging from 500 nm to 2500 nm is realized. The long-wavelength edge extends into the high-loss region of silica fibers. As the length of the PCF is increased, the generated supercontinuum exhibits slightly better coverage in the visible region; however, its coverage in the long-wavelength region is significantly reduced due to the larger absorption loss. Moreover, the output power also suffers from a substantial reduction, as the length of the PCF is increased. With 8 m PCF, the highest power of the generated supercontinuum is only 4.55 W. In this work, for optimizing the overall performance of the system, the length of the PCF is determined to be 1.4 m.

To expand the coverage of the supercontinuum source into the mid-IR region, an HNLF with a ZDW (1550 nm) matched with the 1.5 μm pump is used as the second nonlinear medium. The HNLF is cascaded with the 1.4 m PCF. The residual 1.5 μm pump sent out from the PCF plays an important role in the supercontinuum generation in the HNLF. The supercontinuum experiences a further broadening in the HNLF, particularly in the long-wavelength region. The output characteristics of the supercontinuum acquired after the HNLF are present in Table 1 and Fig. 4. In experiments, we tested a number of fiber lengths for the HNLF. It is found that the performance of the generated supercontinuum (both the spectrum and the output power) deteriorates dramatically with the increase of the fiber length. This can be attributed to the large absorption loss induced by the longer fiber. As the length of the HNLF is 0.2 m, the supercontinuum generated from the system reaches the optimized performance, as shown in Fig. 4(b). Compared

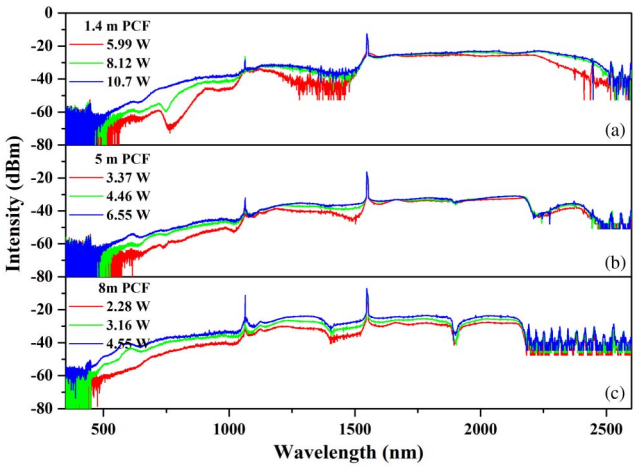

Fig. 3. Spectral evolution of the supercontinuum measured after (a) 1.4 m, (b) 5 m, and (c) 8 m PCF.

Table 1. Characteristics of the Supercontinuum Measured After Various Lengths of HNLF.

Length HNLF (m)	Wavelength range (nm)	Output power (W)
10	890–2600	4.14
4	810–2700	5.62
1	650–2800	7.80
0.2	500–3000	9.01

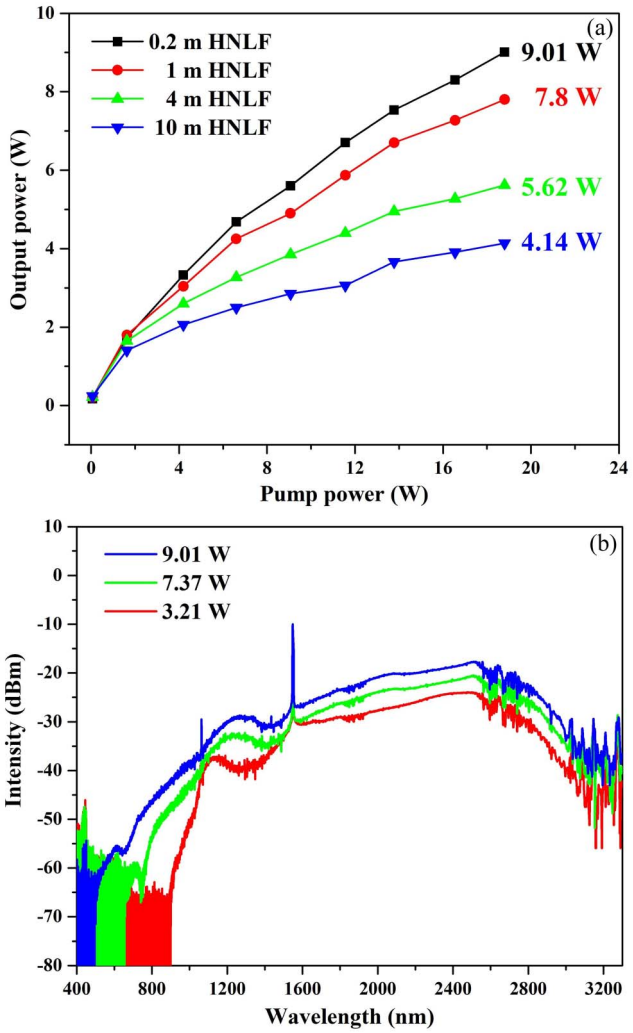

Fig. 4. (a) Output power of the generated supercontinuum measured after different lengths of HNLF as a function of the pump power. (b) Spectral evolution of the generated supercontinuum measured after 0.2 m HNLF.

with the supercontinuum acquired immediately after the 1.4 m PCF, the long-wavelength edge of the supercontinuum acquired after the 0.2 m HNLF is expanded to 3000 nm, and the output power (9.01 W) only shows a small reduction. After the system is warmed up for 20 min, the output power fluctuation is less than 1.4% in 2 h. Moreover, the supercontinuum acquired after the 0.2 m HNLF exhibits an almost identical coverage in the visible region with the supercontinuum acquired after the PCF, with a short-wavelength edge located around 500 nm. Since the visible part is at the edge of the supercontinuum spectrum, the intensity of the spectrum is low. In the next step, we plan to optimize the power of the 1 μm pump source in the system to enhance the visible part of the supercontinuum.

4. Conclusion

To conclude, we experimentally demonstrate a high-power, ultra-broadband supercontinuum source. The supercontinuum generation is realized by pumping cascaded PCF-HNLFs using a 1/1.5 μm dual-band MOPA system. The source achieves a maximum output power of 9.01 W, and its spectral coverage ranges from 500 nm to 3000 nm. As far as we know, this is the highest power ever achieved from a supercontinuum source spanning from visible to mid-IR.

Acknowledgement

This work was supported by the National Natural Science Foundation of China (NSFC) (Nos. 61975136, 61935014, 61775146, and 61905151), the Outstanding Young Teacher Cultivation Projects in Guangdong Province (No. YQ2015142), the Guangdong Basic and Applied Basic Research Foundation (No. 2019A1515010699), the Shenzhen Science and Technology Project (Nos. JCYJ20160520161351540, JCYJ20170817100639177, JCYJ20170302151146995, and JCYJ20160328144942069), the Engineering Applications of Artificial Intelligence Technology Laboratory Project (No. PT201701), and the National Key Research and Development Program of China (No. 2016YFA0401100).

†These authors contributed equally to this work.

References

1. V. V. Alexander, Z. Shi, M. N. Islam, K. Ke, G. Kalinchenko, M. J. Freeman, A. Ifarraguerri, J. Meola, A. Absi, and J. Leonard, "Field trial of active remote sensing using a high-power short-wave infrared supercontinuum laser," Appl. Opt. **52**, 6813 (2013).
2. C. R. Petersen, N. Prtljaga, M. Farries, J. Ward, B. Napier, G. R. Lloyd, J. Nallala, N. Stone, and O. Bang, "Mid-infrared multispectral tissue imaging using a chalcogenide fiber supercontinuum source," Opt. Lett. **43**, 999 (2018).
3. N. Nishizawa, H. Kawagoe, M. Yamanaka, M. Matsushima, K. Mori, and T. Kawabe, "Wavelength dependence of ultrahigh-resolution optical coherence tomography using supercontinuum for biomedical imaging," IEEE J. Sel. Top. Quantum Electron. **25**, 7101115 (2018).
4. N. M. Israelsen, C. R. Petersen, A. Barh, D. Jain, M. Jensen, G. Hannesschläger, P. Tidemand-Lichtenberg, C. Pedersen, A. Podoleanu, and O. Bang, "Real-time high-resolution mid-infrared optical coherence tomography," Light Sci. Appl. **8**, 11 (2019).
5. H. T. Bekman, J. Van Den Heuvel, F. Van Putten, and R. Schleijpen, "Development of a mid-infrared laser for study of infrared countermeasures techniques," Proc. SPIE **5615**, 27 (2004).
6. S. Chen, W. Hu, Y. Xu, Y. Cai, Z. Wang, and Z. Zhang, "Mode-locked pulse generation from an all-FMF ring laser cavity," Chin. Opt. Lett. **17**, 121405 (2019).
7. K. Yao Lau, P. Jern Ker, A. F. Abas, M. T. Alresheedi, and M. A. Mahdi, "Mode-locked fiber laser in the C-band region for dual-wavelength ultrashort pulses emission using a carbon nanotube saturable absorber," Chin. Opt. Lett. **17**, 051401 (2019).
8. K. K. Chen, S. U. Alam, J. H. V. Price, J. R. Hayes, and D. Lin, "Picosecond fiber MOPA pumped supercontinuum source with 39 W output power," Opt. Express **18**, 5426 (2010).
9. X. Hu, W. Zhang, Z. Yang, Y. Wang, and D. Shen, "High average power, strictly all-fiber supercontinuum source with good beam quality," Opt. Lett. **36**, 2659 (2011).
10. S. Gao, Y. Wang, R. Sun, H. Li, C. Tian, D. Jin, and P. Wang, "Ultraviolet-enhanced supercontinuum generation in uniform photonic crystal fiber pumped by a giant-chirped fiber laser," Opt. Express **22**, 24697 (2014).
11. W. Nan, J. H. Cai, Q. Xue, S. P. Chen, L. J. Yang, and H. Jing, "Ultraviolet-enhanced supercontinuum generation with a mode-locked Yb-doped fiber laser operating in dissipative-soliton-resonance region," Opt. Express **26**, 1689 (2018).
12. X. Zou, J. Qiu, X. Wang, Z. Ye, C. Sun, T. Ge, and J. Wu, "An all-fiber supercontinuum source with 30.6-W high-power and ultrawide spectrum ranging from 385 nm to beyond 2400 nm," IEEE Photon. J. **9**, 1502107 (2017).
13. X. Qi, S. Chen, Z. Li, T. Liu, and J. Hou, "High-power visible-enhanced all-fiber supercontinuum generation in a seven-core photonic crystal fiber pumped at 1016 nm," Opt. Lett. **43**, 1019 (2018).
14. H. Chen, Z. Chen, S. Chen, J. Hou, and Q. Lu, "Hundred-watt-level, all-fiber-integrated supercontinuum generation from photonic crystal fiber," Appl. Phys. Express **6**, 032702 (2013).
15. J. Nicholson, A. D. Yablon, P. S. Westbrook, K. S. Feder, and M. F. Yan, "High power, single mode, all-fiber source of femtosecond pulses at 1550 nm and its use in supercontinuum generation," Opt. Express **12**, 3025 (2004).
16. C. Xia, M. Kumar, M.-Y. Cheng, O. P. Kulkarni, M. N. Islam, A. Galvanauskas, J. Terry, F. L. M. J. Freeman, D. A. Nolan, and W. A. Wood, "Supercontinuum generation in silica fibers by amplified nanosecond laser diode pulses," IEEE J. Sel. Top. Quantum Electron. **13**, 789 (2007).
17. C. Xia, X. Zhao, M. N. Islam, F. L. Terry, and J. Mauricio, "10.5 W time-averaged power mid-IR supercontinuum generation extending beyond 4 m with direct pulse pattern modulation," IEEE J. Sel. Top. Quantum Electron. **15**, 422 (2009).
18. K. Yin, B. Zhang, J. Yao, L. Yang, S. Chen, and J. Hou, "Highly stable, monolithic, single-mode mid-infrared supercontinuum source based on low-loss fusion spliced silica and fluoride fibers," Opt. Lett. **41**, 946 (2016).
19. Z. Zheng, D. Ouyang, J. Zhao, M. Liu, S. Ruan, P. Yan, and J. Wang, "Scaling all-fiber mid-infrared supercontinuum up to 10 W-level based on thermal-spliced silica fiber and ZBLAN fiber," Photon. Res. **4**, 135 (2016).
20. Y. Ke, B. Zhang, L. Yang, and H. Jing, "15.2 W spectrally flat all-fiber supercontinuum laser source with >1 W power beyond 3.8 μm," Opt. Lett. **42**, 2334 (2017).
21. T. Wu, L. Yang, Z. Dou, K. Yin, X. He, B. Zhang, and J. Hou, "Ultra-efficient, 10-watt-level mid-infrared supercontinuum generation in fluoroindate fiber," Opt. Lett. **44**, 2378 (2019).
22. D. Jain, R. Sidharthan, P. M. Moselund, S. Yoo, D. Ho, and O. Bang, "Record power, ultra-broadband supercontinuum source based on highly GeO_2 doped silica fiber," Opt. Express **24**, 26667 (2016).
23. D. Jain, R. Sidharthan, G. Woyessa, P. M. Moselund, P. Bowen, S. Yoo, and O. Bang, "Scaling power, bandwidth, and efficiency of mid-infrared supercontinuum source based on a GeO_2-doped silica fiber," J. Opt. Soc. Am. B **36**, A86 (2019).

24. Z. Zheng, D. Ouyang, J. Wang, C. Guo, J. Pei, and S. Ruan, "Supercontinuum generation by using a highly germania-doped fiber with a high-power proportion beyond 2400 nm," IEEE Photon. J. **11**, 3200508 (2019).
25. H. Chen, X. Jiang, S. Xu, and H. Zhang, "Recent progress in multi-wavelength fiber lasers: principles, status, and challenges," Chin. Opt. Lett. **18**, 041405 (2020).
26. X. Ge, J. Yu, W. Liu, S. Ruan, C. Guo, Y. Chen, P. Yan, and P. Hua, "High-power all-fiber 1.0/1.5 μm dual-band pulsed MOPA source," Chin. Opt. Lett. **16**, 020010 (2018).
27. C. Guo, S. Ruan, P. Yan, E. Pan, and H. Wei, "Flat supercontinuum generation in cascaded fibers pumped by a continuous wave laser," Opt. Express **18**, 11046 (2010).